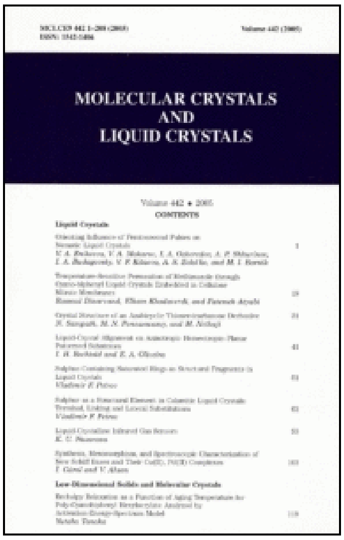

Molecular Crystals and Liquid Crystals
Publication details, including instructions for authors and subscription information:
http://www.informaworld.com/smpp/title~content=t713644168

Ferrocene-Based Rod-Like Mesogens Terminated with Oxadiazole Unit

K. C. Majumdar[a]; P. K. Shyam[a]
[a] Department of Chemistry, University of Kalyani, Kalyani, West Bengal, India

To cite this Article Majumdar, K. C. and Shyam, P. K.(2010) 'Ferrocene-Based Rod-Like Mesogens Terminated with Oxadiazole Unit', Molecular Crystals and Liquid Crystals, 528: 1, 3 — 9

To link to this Article: DOI: 10.1080/15421406.2010.504503

URL: http://dx.doi.org/10.1080/15421406.2010.504503

Mol. Cryst. Liq. Cryst., Vol. 528: pp. 3–9, 2010

ISSN: 1542-1406 print/1563-5287 online
DOI: 10.1080/15421406.2010.504503

Taylor & Francis
Taylor & Francis Group

Ferrocene-Based Rod-Like Mesogens Terminated with Oxadiazole Unit

K. C. MAJUMDAR AND P. K. SHYAM

Department of Chemistry, University of Kalyani, Kalyani,
West Bengal, India

A series of ferrocene-based rod-like mesogens has been synthesized in which the oxadiazole unit is in a terminal position. The length of the terminal S-alkyl chain, alkyl spacer length, and substitution on lateral position have been varied. All the synthesized compounds are thermally stable and exhibit mesomorphism. Most of them display two enantiotropic mesophases nematic-smectic C. Only one compound exhibits enantiotropic smectic C phase.

Keywords Ferrocene; N; oxadiazole; Schiff's base; SmC

Introduction

For the last few years, there has been considerable interest in liquid crystals containing organometallic components that combine properties of the metals with those of the mesogenic moieties because this could lead to processable materials with interesting anisotropic optical, electronic, and magnetic properties [1,2]. Because ferrocene possesses unique redox characteristics, it is used as a valuable unit for switchable system and nowadays electron transfer is used to generate mesomorphism in the ferrocene-ferrocenium redox system [3]. The first liquid crystals containing a transition metal were prepared ferrocene monoesters reported by Malthête and Billard [4]. Nevertheless, most of the ferrocene-based liquid-crystalline materials are based on 1,1′-disubstituted ferrocene [5]. Limited studies in the direction of monosubstituted ferrocene derivatives are attributed to the fact that monosubstituted ferrocenes, because of their unfavorable molecular shape (L-shape) and due to repulsive steric effects of the ferrocene units, which hinders the ability of the molecules to pack in layers, thus favoring the formation of a nematic phase. However, introduction of ferrocene units as components of chiral liquid-crystalline materials results in high thermal stability and other additional properties, among which its ability to undergo reversible one-electron transfer processes is important. There are few examples of chiral liquid-crystalline materials containing ferrocene units at the terminal position that exhibit a wide range of phases (SmA, SmC*, N*, TGB, etc.) [6].

Address correspondence to K. C. Majumdar, Department of Chemistry, University of Kalyani, Kalyani, West Bengal 741235, India. E-mail: kcm_ku@yahoo.co.in

On the other hand, the 1,3,4-oxadiazoles are interesting systems for the design and synthesis of liquid-crystalline compounds with a classical rod-like structure. The 1,3,4-oxadiazole derivatives are well known for their high thermal and hydrolytic stability, resistance to oxidative degradation, and electron-accepting properties [7]. Some groups used an oxadiazole ring either in the central position or in a terminal position of the mesogenic rigid core and some used these units as a central core of banana-shaped light-emitting liquid-crystalline materials [8].

In continuation of our efforts to synthesize ferrocene-based liquid-crystalline materials [9] we undertook a study to synthesize ferrocene-based rod-like mesogen terminated with an oxadiazole unit. Here we report our results.

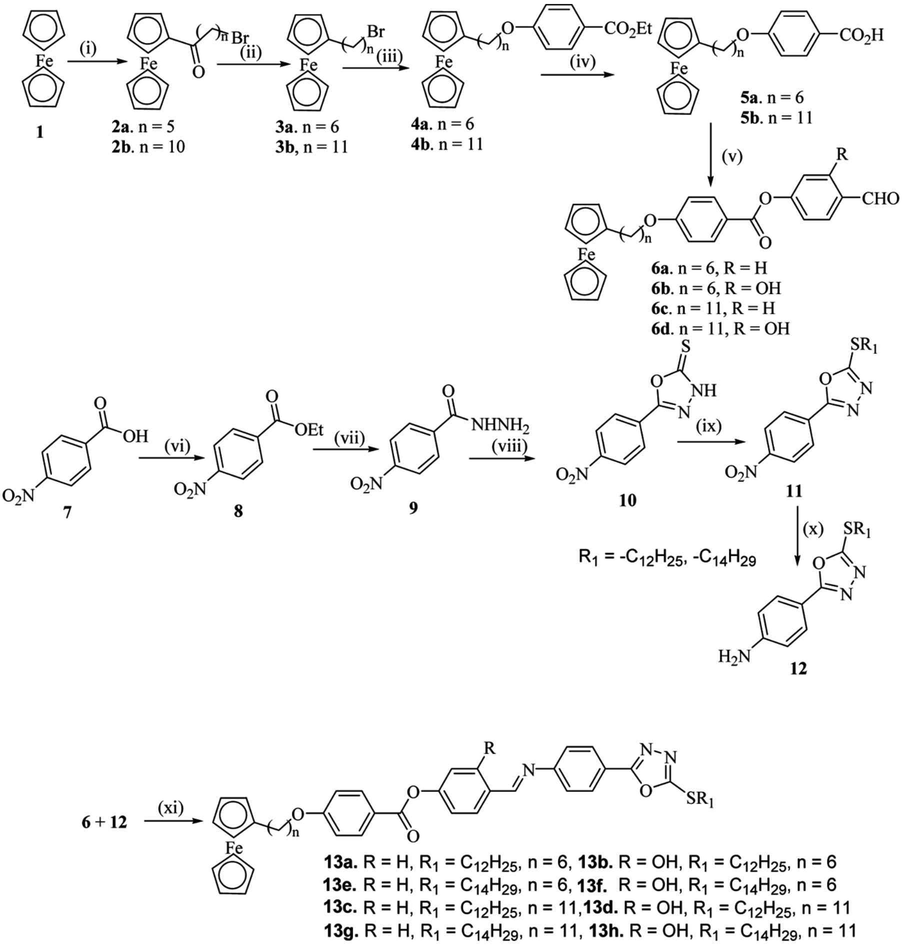

Scheme 1. *Reagents and conditions*: (i) 6-bromohexanoyl chloride/11-bromodecanoyl chloride, $AlCl_3$, $CHCl_3$, rt, 2 h; (ii) Zn-Hg, conc. HCl, benzene–water, reflux, 20–24 h; (iii) *p*-hydroxyethylbenzoate, acetone, K_2CO_3, reflux, 12 h; (iv) C_2H_5OH, KOH, reflux, 2 h; (v) *p*-hydroxybenzaldehyde/2,4-dihydroxybenzaldehyde, DCC, DMAP, $CHCl_3$, rt, 1–2 h; (vi) ethanol, H_2SO_4, (2 mL), reflux, 2 days; (vii) $NH_2NH_2 \cdot H_2O$, ethanol, reflux, 2 h; (viii) ethanol, KOH, CS_2, rt; (ix) R_1Br, Et_3N, ethanol, reflux, 4 h; (x) $SnCl_2 \cdot H_2O$, ethylacetate, reflux, 6 h; (xi) dry ethanol, acetic acid (cat), reflux, 24 h.

Ferrocene was first converted to either 6-bromohexanoyl ferrocene (**2a**) or 11-bromodecanoyl ferrocene (**2b**) by treatment with respective acid chlorides in dry chloroform in the presence of anhydrous aluminum chloride. The compound **2a** or **2b** on treatment with zinc amalgam in the presence of concentrated hydrochloric acid in benzene–water under refluxing conditions afforded compound **3a** or **3b**. Compound **3a** or **3b** upon reaction with *p*-hydroxyethylbenzoate and anhydrous potassium carbonate in refluxing acetone and subsequent hydrolysis of the resulting ester with ethanolic potassium hydroxide afforded the acid derivative **5a** or **5b**. The acid derivatives on esterification with different hydroxybenzaldehydes gave the corresponding ester aldehyde derivatives **6a-d**.

On the other hand, *p*-nitrobenzoic acid **7** was converted to its ethylbenzoate derivative **8** with acidic ethanol under refluxing condition. The ester derivative **8** on treatment with hydrazine hydrate afforded the compound **9**, which cyclized readily to give **10**. S-alkylation of **10** with alkyl bromide and subsequent hydrogenation of its S-alkylated derivative gave the amine **12**. The aldehydes **6** and amines **12** on condensation afforded a series of Schiff's bases **13a-f** (Scheme 1).

Results and Discussion

The thermal behaviors and liquid-crystalline properties of the compounds **13a-h** were investigated by differential scanning calorimetry (DSC) and polarized optical microscopy (POM). The transition temperatures and associated enthalpies calculated from DSC experiments are summarized in Table 1.

From the DSC experiments it is quite clear that all the compounds exhibit two mesophase transitions both in heating as well as in cooling cycles except compound **13b**, which exhibit an extra transition in the heating cycle probably due to solid–solid transition and **13h**, which shows only one mesophase transition in both the cycles.

Table 1. Transition temperature (°C) and associated enthalpy (KJ/Mol) calculated from DSC thermogram

13a	$\mathrm{Cr} \xrightarrow[(48.5)]{123.3} \mathrm{SmC} \xrightarrow[(1.59)]{170.6} \mathrm{N} \xrightarrow[(0.78)]{187.1} \mathrm{I} \xrightarrow[(0.89)]{184.9} \mathrm{N} \xrightarrow[(1.46)]{167.9} \mathrm{SmC} \xrightarrow[(31.1)]{62.7} \mathrm{Cr}$
13b	$\mathrm{Cr} \xrightarrow[(17.1)]{104.0} \mathrm{Cr_1} \xrightarrow[(38.2)]{131.6} \mathrm{SmC} \xrightarrow[(3.80)]{194.1} \mathrm{N} \xrightarrow[(0.87)]{203.2} \mathrm{I} \xrightarrow[(0.80)]{199.0} \mathrm{N} \xrightarrow[(2.10)]{189.0} \mathrm{SmC} \xrightarrow[(35.5)]{113.8} \mathrm{Cr}$
13c	$\mathrm{Cr} \xrightarrow[(71.8)]{111.3} \mathrm{SmC} \xrightarrow[(3.12)]{174.7} \mathrm{N} \xrightarrow[(1.03)]{180.4} \mathrm{I} \xrightarrow[(1.03)]{179.1} \mathrm{N} \xrightarrow[(3.04)]{173.4} \mathrm{SmC} \xrightarrow[(37.9)]{70.9} \mathrm{Cr}$
13d	$\mathrm{Cr} \xrightarrow[(42.5)]{128.3} \mathrm{SmC} \xrightarrow[(5.39)]{195.3} \mathrm{N} \xrightarrow[(0.79)]{197.4} \mathrm{I} \xrightarrow[(0.79)]{195.0} \mathrm{N} \xrightarrow[(4.18)]{192.8} \mathrm{SmC} \xrightarrow[(40.3)]{113.3} \mathrm{Cr}$
13e	$\mathrm{Cr} \xrightarrow[(52.9)]{120.0} \mathrm{SmC} \xrightarrow[(0.97)]{170.4} \mathrm{N} \xrightarrow[(0.84)]{183.9} \mathrm{I} \xrightarrow[(1.12)]{182.9} \mathrm{N} \xrightarrow[(0.86)]{169.1} \mathrm{SmC} \xrightarrow[(38.0)]{84.4} \mathrm{Cr}$
13f	$\mathrm{Cr} \xrightarrow[(46.7)]{149.3} \mathrm{SmC} \xrightarrow[(4.07)]{194.7} \mathrm{N} \xrightarrow[(1.03)]{200.4} \mathrm{I} \xrightarrow[(0.66)]{197.6} \mathrm{N} \xrightarrow[(3.20)]{191.3} \mathrm{SmC} \xrightarrow[(42.9)]{128.5} \mathrm{Cr}$
13g	$\mathrm{Cr} \xrightarrow[(53.7)]{100.8} \mathrm{SmC} \xrightarrow[(2.65)]{173.4} \mathrm{N} \xrightarrow[(0.83)]{177.0} \mathrm{I} \xrightarrow[(0.97)]{175.4} \mathrm{N} \xrightarrow[(2.76)]{171.6} \mathrm{SmC} \xrightarrow[(25.8)]{69.1} \mathrm{Cr}$
13h	$\mathrm{Cr} \xrightarrow[(40.1)]{120.5} \mathrm{SmC} \xrightarrow[(7.92)]{193.7} \mathrm{I} \xrightarrow[(5.97)]{191.3} \mathrm{SmC} \xrightarrow[(34.1)]{112.0} \mathrm{Cr}$

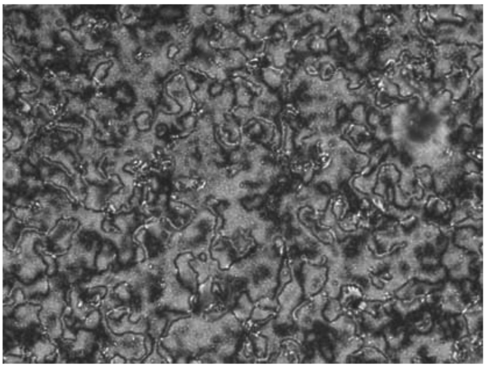

Figure 1. POM picture of **13a** at 184°C.

All the phase transitions are enantiotropic in nature. Compounds possessing a lateral hydroxyl group attached to the aromatic ring exhibit the same phase transitional behaviors in respect to the other compounds (except **13h**) of the series but possess higher transition temperature and a high value of enthalpy change due to the presence of intramolecular hydrogen bonding. Compounds having the same spacer length and melting as well as clearing temperature decrease with the increase in the S-alkyl chain length. The change in the spacer length also has a similar effect as above. On slow cooling from the isotropic phase of the compound **13a**, small droplets are seen that readily transform into the thread-like texture characteristics of the N phase (Fig. 1). On further cooling, a phase transition occurs at around 167°C, after which a Schlieren texture with only four point brushes appears due to the optical biaxial nature of the SmC phase (Fig. 2). On further cooling, the sample solidifies. All the other compounds except **13h** exhibit a similar type of phase behavior under POM observation. Compound **13h** shows a direct transition to the SmC phase from isotropic melt when cooled slowly during POM observation. Compounds **13a-h** are not transparent to X-ray (the reason is uncertain), and therefore diffraction patterns could not be recorded.

Parra *et al.* [8a] reported a series of achiral amides, achiral Schiff's bases, chiral amides, and chiral Schiff's bases incorporating a 1,3,4-oxadiazole ring. Some of the

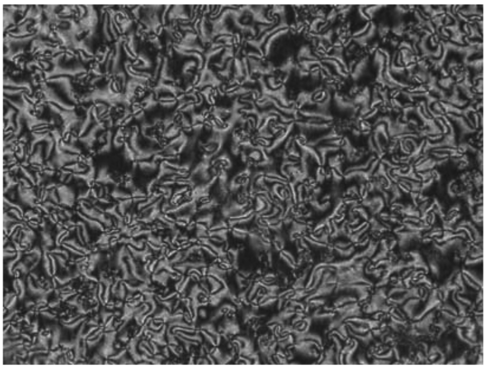

Figure 2. POM picture of **13a** at 165°C.

compounds of this series do not exhibit mesomorphic phases. Most of the achiral compounds containing Schiff''s base linkage display an enantiotropic dimorphism SmC-SmA or SmA-N whereas the chiral compounds show only a chiral SmC phase. There are many examples of liquid-crystalline compounds having disubstitution on the oxadiazole ring, but those compounds are bent in nature [8b,8c]. Very few examples are known where disubstituted oxadiazole rings are used to synthesize rod-shaped liquid-crystalline compounds [8a]. On the other hand, Loubser and Imrie [10] have synthesized a series of ester derivatives containing monosubstituted ferrocene. They observed that the size and shape of the aromatic core of the substituent on ferrocene play an important role in determining the thermal properties of these compounds. According to Loubser and Imrie [10], a minimum of three rings in the substituent core is necessary for stabilizing the nematic phase, but four rings vastly enhances the nematic behavior. Carlesen *et al.* [11] synthesized some mono substituted ferrocene-containing liquid-crystalline materials having three aromatic rings and observed either monotropic or enantiotropic smectic phase behavior. Seshadri and Haupt [6a] reported a monosubstituted ferrocene-based metallomesogen with a chiral Schiff's base with long Sc* domain, a TGBA phase in between SmA and N*, and a blue phase just before the clearing point, in spite of a bulky pendant ferrocene unit on the other side and a relatively small terminal group appended to the chiral center on the other side. We too have reported [6b] some chiral cholesterol-based liquid-crystalline material terminated with a ferrocenyl moiety. These dimers have been prepared by varying either the number of aromatic rings, the spacer between the phenyl rings and the ferrocenyl unit, and introducing lateral substitution. Most of the dimers exhibited the the N* phase over a wide temperature range and two of the dimers showed SmA and/or SmA, TGB in addition to the N* phase.

In the present study, we have synthesized a series of ferrocene-based liquid-crystalline material terminated with an oxadiazole ring. All the synthesized compounds are liquid-crystalline in nature and exhibit either an enantiotropic SmC phase or enantiotropic N-SmC transition. To our best of our knowledge, this may the first example of ferrocene-based rod-like liquid-crystalline materials that terminated with an oxadiazole ring. All the compounds contain two aromatic rings. Therefore, the occurrence of an N-SmC transition in this study is interesting.

General Procedure for the Preparation of Compounds 6a-d

All the compounds were prepared according to the published procedure [6b].

General Procedure for the Preparation of Compounds 12

Compounds **12** were prepared according to the published procedure [12].

General Procedure for the Preparation of the Schiff's Bases 13a-h

Compound **6a** (100 mg, 0.196 mmol) was dissolved in dry hot ethanol (3 mL) and a catalytic amount of glacial acetic acid was added. To this solution, amine derivative **12a** (71 mg, 0.196 mmol) dissolved in dry hot ethanol (5 mL) was added drop wise. After 4–6 h a pale yellow solid material separated out, which was filtered in hot condition and washed three times with hot ethanol (3 × 5 mL) to give a solid as a pure compound **13a**. Similarly, compounds **13b-h** were prepared.

*Compound **13a***. Yield 80% (pale yellow solid); IR ν_{max} 2926, 1736, 1623, 1601 cm^{-1}; ^{1}H NMR (400 MHz, $CDCl_3$): δ_H 0.86–1.87 (m, 31H), 2.35 (t, 2H, $J = 7.6$ Hz), 3.30 (t, 2H, $J = 7.2$ Hz), 4.04–4.07 (m, 6H), 4.09 (s, 5H), 6.98 (d, 2H, $J = 8.8$ Hz), 7.29 (d, 2H, $J = 8.4$ Hz), 7.35 (d, 2H, $J = 8.4$ Hz), 7.98 (d, 2H, $J = 8.8$ Hz), 8.03 (d, 2H, $J = 8.8$ Hz), 8.15 (d, 2H, $J = 8.8$ Hz), 8.48 (s, 1H). ^{13}C NMR (125 MHz, $CDCl_3$): δ_C 14.1, 22.7, 25.9, 28.6, 29.1, 29.3, 29.3, 29.4, 29.5, 29.6, 31.1, 31.9, 32.7, 67.1, 68.1, 68.3, 68.5, 89.2, 114.4, 121.1, 121.2, 121.6, 122.4, 122.6, 127.8, 128.3, 130.3, 131.2, 132.4, 133.4, 153.9, 154.8, 160.3, 163.7, 164.4, 164.5, 165.5. Anal. Calcd. for $C_{50}H_{59}FeN_3O_4S$: C, 70.33; H, 6.96; N, 4.92%. Found: C, 70.50; H, 6.99; N, 4.98%.

*Compound **13b***. Yield 85% (yellow solid); IR (KBr): ν_{max} 2924, 1741, 1624, 1603 cm^{-1}; ^{1}H NMR (400 MHz, $CDCl_3$): δ_H 0.86–1.87 (m, 31H), 2.35 (t, 2H, $J = 7.6$ Hz), 3.31 (t, 2H, $J = 7.2$ Hz), 4.04–4.06 (m, 6H), 4.09 (s, 5H), 6.85 (d, 1H, $J = 8.0$ Hz), 6.92 (s, 1H), 6.97 (d, 2H, $J = 8.8$ Hz), 7.38 (d, 2H, $J = 8.4$ Hz), 7.46 (d, 1H, $J = 8.4$ Hz), 8.07 (d, 2H, $J = 8.0$ Hz), 8.13 (d, 2H, $J = 8.8$ Hz), 8.68 (s, 1H), 13.24 (s, 1H); Anal. Calcd. for $C_{50}H_{59}FeN_3O_5S$: C, 69.03; H, 6.84; N, 4.83%. Found: C, 69.23; H, 6.90; N, 4.91%.

*Compound **13c***. Yield 75% (pale yellow solid); IR (KBr): ν_{max} 2919, 1731, 1626, 1606 cm^{-1}; ^{1}H NMR (400 MHz, $CDCl_3$): δ_H 0.86–1.88 (m, 41H), 2.31 (t, 2H, $J = 7.6$ Hz), 3.30 (t, 2H, $J = 7.2$ Hz), 4.03–4.09 (m, 6H), 4.13 (s, 5H), 6.97 (d, 2H, $J = 8.8$ Hz), 7.29 (d, 2H, $J = 8.4$ Hz), 7.35 (d, 2H, $J = 8.8$ Hz), 7.98 (d, 2H, $J = 8.8$ Hz), 8.03 (d, 2H, $J = 8.4$ Hz), 8.14 (d, 2H, $J = 8.8$ Hz), 8.48 (s, 1H). Anal. Calcd. for $C_{55}H_{69}FeN_3O_4S$: C, 71.49; H, 7.53; N, 4.55%. Found: C, 71.67; H, 7.62; N, 4.64%.

*Compound **13d***. Yield 90% (yellow solid); IR (KBr): ν_{max} 2920, 1736, 1625, 1603 cm^{-1}; ^{1}H NMR (400 MHz, $CDCl_3$): δ_H 0.87–1.87 (m, 41H), 2.31 (t, 2H, $J = 7.6$ Hz), 3.31 (t, 2H, $J = 7.2$ Hz), 4.03–4.08 (m, 6H), 4.09 (s, 5H), 6.85 (d, 1H, $J = 8.4$ Hz), 6.91 (s, 1H), 6.97 (d, 2H, $J = 8.8$ Hz), 7.38 (d, 2H, $J = 8.4$ Hz), 7.46 (d, 1H, $J = 8.8$ Hz), 8.06 (d, 2H, $J = 8.4$ Hz), 8.13 (d, 2H, $J = 9.2$ Hz), 8.68 (s, 1H), 13.24 (s, 1H). Anal. Calcd. for $C_{55}H_{69}FeN_3O_5S$: C, 70.27; H, 7.40; N, 4.47%. Found: C, 70.50; H, 7.49; N, 4.55%.

*Compound **13e***. Yield 86% (pale yellow solid); IR (KBr): ν_{max} 2926, 1736, 1623, 1601 cm^{-1}; ^{1}H NMR (400 MHz, $CDCl_3$): δ_H 0.88–1.89 (m, 35H), 2.35 (t, 2H, $J = 7.2$ Hz), 3.30 (t, 2H, $J = 7.2$ Hz), 4.04–4.07 (m, 6H), 4.10 (s, 5H), 6.98 (d, 2H, $J = 8.8$ Hz), 7.29 (d, 2H, $J = 8.4$ Hz), 7.35 (d, 2H, $J = 8.4$ Hz), 7.98 (d, 2H, $J = 8.4$ Hz), 8.03 (d, 2H, $J = 8.4$ Hz), 8.15 (d, 2H, $J = 8.8$ Hz), 8.48 (s, 1H). Anal. Calcd. for $C_{52}H_{63}FeN_3O_4S$: C, 70.81; H, 7.20; N, 4.76%. Found: C, 70.92; H, 7.29; N, 4.81%.

*Compound **13f***. Yield 78% (yellow solid); IR (KBr): ν_{max} 2921, 1724, 1623, 1602 cm^{-1}; ^{1}H NMR (400 MHz, $CDCl_3$): δ_H 0.86–1.83 (m, 35H), 2.35 (t, 2H, $J = 7.2$ Hz), 3.31 (t, 2H, $J = 7.2$ Hz), 4.04–4.06 (m, 6H), 4.09 (s, 5H), 6.85 (d, 1H, $J = 8.0$ Hz), 6.92 (s, 1H), 6.97 (d, 2H, $J = 8.8$ Hz), 7.39 (d, 2H, $J = 7.6$ Hz), 7.46 (d, 1H, $J = 8.4$ Hz), 8.07 (d, 2H, $J = 7.6$ Hz), 8.13 (d, 2H, $J = 8.8$ Hz), 8.68 (s, 1H), 13.26 (s, 1H). Anal. Calcd. for $C_{52}H_{63}FeN_3O_5S$: C, 69.55; H, 7.07; N, 4.68%. Found: C, 69.75; H, 7.18; N, 4.76%.

*Compound **13g***. Yield 95% (pale yellow solid); IR (KBr): ν_{max} 2919, 1729, 1628, 1604 cm^{-1}; ^{1}H NMR (400 MHz, $CDCl_3$): δ_H 0.86–1.86 (m, 45H), 2.31 (t, 2H,

$J = 7.6$ Hz), 3.30 (t, 2H, $J = 7.2$ Hz), 4.03–4.05 (m, 6H), 4.07 (s, 5H), 6.97 (d, 2H, $J = 8.8$ Hz), 7.29 (d, 2H, $J = 8.4$ Hz), 7.35 (d, 2H, $J = 8.4$ Hz), 7.98 (d, 2H, $J = 8.8$ Hz), 8.03 (d, 2H, $J = 8.4$ Hz), 8.14 (d, 2H, $J = 8.8$ Hz), 8.48 (s, 1H). Anal. Calcd. for $C_{57}H_{73}FeN_3O_4S$: C, 71.90; H, 7.73; N, 4.41%. Found: C, 72.06; H, 7.85; N, 4.51%.

Compound ***13h***. Yield 90% (yellow solid); IR (KBr): ν_{max} 2920, 1736, 1624, 1603 cm^{-1}; ^1H NMR (400 MHz, $CDCl_3$): δ_H 0.87–1.88 (m, 45H), 2.31 (t, 2H, $J = 7.2$ Hz), 3.31 (t, 2H, $J = 7.2$ Hz), 4.03–4.07 (m, 6H), 4.13 (s, 5H), 6.85 (d, 1H, $J = 8.4$ Hz), 6.92 (s, 1H), 6.97 (d, 2H, $J = 9.2$ Hz), 7.38 (d, 2H, $J = 8.4$ Hz), 7.46 (d, 1H, $J = 8.4$ Hz), 8.07 (d, 2H, $J = 8.0$ Hz), 8.13 (d, 2H, $J = 8.8$ Hz), 8.68 (s, 1H), 13.24 (s, 1H). Anal. Calcd. for $C_{57}H_{73}FeN_3O_5S$: C, 70.72; H, 7.60; N, 4.34%. Found: C, 70.86; H, 7.69; N, 4.38%.

Acknowledgment

We thank the Department of Science and Technology (New Delhi) for financial assistance. P. K. Shyam is grateful to the Council of Scientific and Industrial Research (New Delhi) for Fellowship.

References

[1] (a) Deschenaux, R., & Goodby, J. W. (1995). Ferrocene-continuing thennotropic liquid crystals. In: *Ferrocenes*, Togni, A. & Hayashi, T. (Eds.), VCH: Weinheim, (b) Zanello, P. (1995). Electrochemical and X-ray structural aspects of transition metal complexes containing redox-active ferrocene ligands. In: *Ferrocenes*, Togni, A. & Hayashi, T. (Eds.), VCH: Weinheim.

[2] (a) Deschenaux, R., Kosztics, I., Scholten, U., Guillon, D., & Ibn-Elhaj, M. (1994). *J. Mater. Chem.*, *4*, 1351; (b) Deschenaux, R., Jauslin, I., Scholten, U., Turpin, F., Guillon, D., & Heinrich, B. (1998). *Macromolecules*, *31*, 5647; (c) Deschenaux, R., Turpin, F., & Guillon, D. (1997). *Macromolecules*, *30*, 3759.

[3] Deschenaux, R., Schweissguth, M., & Levelut, A.-M. (1996). *Chem. Comm.*, 1275.

[4] Malthête, J., & Billard, J. (1976). *Mol. Cryst. Liq. Cryst. Lett.*, *34*, 117.

[5] Imrie, C., & Loubser, C. (1994). *J. Chem. Soc. Chem. Comm.*, 2159.

[6] (a) Seshadri, T., & Haupt, H.-J. (1998). *Chem. Comm.*, 735; (b) Majumdar, K. C., Chakravorty, S., Pal, N., & Sinha, R. K. (2009). *Tetrahedron*, *65*, 7998.

[7] Cristiano, R., Vieira, A. A., Ely, F., & Gallardo, H. (2006). *Liq. Cryst.*, *33*, 381.

[8] (a) Parra, M. L., Elgueta, E. Y., Jimenez, V., & Hidalgo, P. I. (2009). *Liq. Cryst.*, *36*, 301; (b) Zhu, L.-R., Yao, F., Han, J., Pang, M.-L., & Meng, J.-B. (2009). *Liq. Cryst.*, *36*, 209; (c) He, C. F., Richards, G. T., Kelly, S. M., Contoret, A. E. A., & O'Neil, M. (2007). *Liq. Cryst.*, *34*, 1249.

[9] (a) Majumdar, K. C., Chakravorty, S., Sinha, R. K., & Pal, N. (2009). *Mol. Cryst. Liq. Cryst.*, *515*, 123; (b) Majumdar, K. C., Chakravorty, S., Pal, N., & Rao, N. V. S. (2009). *Tetrahedron*, *65*, 152; (c) Majumdar, K. C., Chattopadhyay, B., Chakravorty, S., Pal, N., & Sinha, R. K. (2008). *Tetrahedron Lett.*, *49*, 7149; (d) Majumdar, K. C., Chakravorty, S., & Pal, N. (2009). *Mol. Cryst. Liq. Cryst.*, *503*, 112; (f) Majumdar, K. C., Sinha, R. K., & Chakravorty, S. (2009). *J. Phys. Chem. Solid.*, *70*, 1171; (g) Majumdar, K. C., Mondal, S., & Sinha, R. K. (2010). *New J. Chem.*, *34*, 1255–1260; (h) Majumdar, K. C., Chattopadhyay, B., Shyam, P. K., & Pal, N. (2009). *Tetrahedron Lett.*, *50*, 6901; (i) Majumdar, K. C., Mondal, S., Pal, N., & Sinha, R. K. (2009). *Tetrahedron Lett.*, *50*, 1992.

[10] Loubser, C., & Imrie, C. (1997). *J. Chem. Soc. Perkin Trans.*, *2*, 399.

[11] Carleseu, I., Hurdue, N., Scutaru, D., Catanescu, O., & Chien, L.-C. (2004). *Electron. Liq. Cryst. Comm.*, 43–37.

[12] Narasimhaswamy, T., & Srinivasan, K. S. V. (2004). *Liq. Cryst.*, *31*, 1457.